## Liquid Crystals

Publication details, including instructions for authors and subscription information:
http://www.informaworld.com/smpp/title~content=t713926090

# Synthesis and mesomorphism study of star-shaped carbohydrate liquid crystals containing glucosyl and glutamyl residues

Baoyan Zhang[a]; Wenqiang Xiao[a]; Yuehua Cong[b]; Yuhong Zhang[a]
[a] The Research Centre for Molecular Science and Engineering, Northeastern University, Shenyang 110004, P. R. China [b] School of Chemistry, Cardiff University, Cardiff, United Kingdom

**To cite this Article** Zhang, Baoyan , Xiao, Wenqiang , Cong, Yuehua and Zhang, Yuhong(2007) 'Synthesis and mesomorphism study of star-shaped carbohydrate liquid crystals containing glucosyl and glutamyl residues', Liquid Crystals, 34: 10, 1129 — 1136

**To link to this Article: DOI:** 10.1080/02678290701658266

**URL:** http://dx.doi.org/10.1080/02678290701658266

*Liquid Crystals*, Vol. 34, No. 10, October 2007, 1129–1136

# Synthesis and mesomorphism study of star-shaped carbohydrate liquid crystals containing glucosyl and glutamyl residues

BAOYAN ZHANG*†, WENQIANG XIAO†, YUEHUA CONG‡ and YUHONG ZHANG†

†The Research Centre for Molecular Science and Engineering, Northeastern University, Shenyang 110004, P. R. China

‡School of Chemistry, Cardiff University, Cardiff, United Kingdom

(*Received 31 May 2007; accepted 31 August 2007*)

A series of novel star-shaped carbohydrate derivative liquid crystals was synthesized with glucose as the chiral core structure. Glutamyl mesogenic moieties, L-*R*-{*n*-[4-(cholesteryloxycarbonyl)benzoyloxy]alkoxy}glutamic acid, were introduced to the five hydroxy groups of glucose by direct esterification. The chemical structures of the target liquid crystalline compounds were confirmed by element analysis and Fourier transform infrared, $^{1}$H NMR and $^{13}$C NMR spectroscopy. The mesomorphic behaviour and thermal properties of target liquid crystalline compounds were investigated with differential scanning calorimetry, thermogravimetric analysis, polarizing optical microscopy, X-ray diffraction and specific rotation. All the target compounds exhibit a cholesteric liquid crystalline phase. These compounds demonstrate a wide mesogenic region and high thermal stability. The effect of flexible spacer group length of the target compounds on the molecular structure and thermal properties is discussed.

## 1. Introduction

Liquid crystals (LCs) are very common and important, mainly because of their unique properties, including the selective reflection of light and ferroelectricity, and their potential applications in numerous areas, especially in the fields of optics, electro-optics, thermoconducting materials and fast switching. Carbohydrates and amino acids are a new yet very promising source for LC synthesis, not only because they form various types of mesomorphous materials, but also because they provide the core structure of glycosides, which are important macromolecules exhibiting liquid crystalline behaviour [1–15].

Although there have been several studies of the synthesis of LCs with long aliphatic chains attached to sugars [16–20], there have been few reports on the synthesis of LCs synthesized by assembling *a*-D-(+)-glucose with mesogenic units containing a glutamic acid chain. In this paper, we report the design and synthesis of a series of novel star-shaped carbohydrate derivative LCs using glucose as the chiral core structure. Glutamyl mesogenic moieties were introduced to the five hydroxy groups of glucose by direct esterification. The azyls in the molecular structure of the target compounds are active groups, which could lead to further synthesis. These star-shaped LCs, termed GG*n*GC (glucose–glutacid–*n*-glycol–cholesterol, where *n* denotes the number of carbon atoms in the glycol), were different compared with traditional LCs.

The chemical structures of GG*n*GC series were characterized with Fourier transform infrared (FTIR), $^{1}$H NMR and $^{13}$C NMR spectroscopy and element analysis. The mesomorphic behaviour and thermal properties were investigated using differential scanning calorimetry (DSC), thermogravimetric analysis (TGA), polarizing optical microscopy (POM), X-ray diffraction (XRD) and specific rotation (SROT). The effect of the flexible spacer group length of the target compounds on the thermal properties and molecular structure is discussed.

## 2. Experimental

### 2.1. *Materials and characterization*

Glutamic acid was purchased from Shanghai Chemical Industry Co (China). Cholesterol was purchased from Henan Xiayi Medical Co (China). Ahydrous *a*-D-(+)-glucose and glycol were purchased from Beijing Jinlong Chemical Reagent (China). *p*-Phthaloyl chloride was purchased from Beijing Fuxing Chemical Industry (China). Chloroform was first washed over water and

---

*Corresponding author. Email: baoyanzhang@hotmail.com

*Liquid Crystals*
ISSN 0267-8292 print/ISSN 1366-5855 online © 2007 Taylor & Francis
http://www.tandf.co.uk/journals
DOI: 10.1080/02678290701658266

then distilled. All other solvents and reagents were purified by standard methods.

The FTIR spectra were measured on a Spectrum One (B) spectrometer (PerkinElmer, Foster City, CA). The elemental analyses were carried out using an Elementar Vario EL III (Elementar, Hanau, Germany). $^1$H NMR and $^{13}$C NMR spectra (300 MHz) were obtained with a Gemini 300 spectrometer (Varian Associates, Palo Alto, CA). SROT was measured on a PerkinElmer 341 polarimeter. Thermodynamic parameters were determined with a DSC 204 (Netzsch, Hanau, Germany) equipped with a liquid nitrogen cooling system. The heating and cooling rates were 10°C min$^{-1}$. The thermal stability of the star-shaped LCs under atmosphere was measured with a Netzsch TGA 209C thermograrimetric analyzer. A DMRX POM instrument (Leica, Germany) equipped with a THMSE-600 hot stage (Linkam, England) was used to observe phase-transition temperatures and analyse liquid crystalline properties through the observation of optical textures. XRD measurements were performed with nickel-filtered Cu-K$_\alpha$ ($\lambda$=1.542 Å) radiation with a DMAX-3A powder diffractometer (Rigaku, Tokyo, Japan).

### 2.2. *Synthesis*

The synthetic routes of the GG*n*GC series and molecular structure of GG4GC are shown in schemes 1 and 2, respectively. In this paper, the synthesis of GG4GC (*n*=4) is chosen as a specific example of the procedure followed.

**2.2.1. *N*-phthaloyl-L-glutamic acid anhydride (B).** The mixture of glutamic acid (14.70 g, 0.1 mol) and *O*-phthalic anhydride (16.30 g, 0.11 mol) was stirred at 180–200°C for 15 min. The mixture was recrystallized from ethanol/water (1:10) to give the corresponding protected acid. The protected glutamic acid (11.10 g, 0.4 mol) in acetic anhydride (25 ml) was stirred at 80°C for 2 h. The precipitated crude product was filtered and then washed by ether to give the pure white solid (8.30 g, 40%), m.p. 160–161°C. IR (KBr, $\nu$ cm$^{-1}$): 1816, 1713, 1608. $^1$ H NMR ($CDCl_3$) $\delta$: 2.03–2.30 (m, 4H), 4.40 (d, 1H, d, *J*=4.2 Hz), 7.93 (d, 2H, d, *J*=6 Hz), 7.96 (m, 2H). $^{13}$ C NMR ($CDCl_3$) $\delta$: 21.86, 29.02, 48.92, 124.32, 132.66, 137.71, 165.51, 165.92, 167.64. Elemental analysis: calculated for $C_{13}H_9NO_5$, C 60.22, H 3.54; found, C 60.10, H 3.32%.

**2.2.2. *N*-phthaloyl-L-*R*-{4-[4-(cholesteryloxycarbonyl) benzoyloxy]butoxy}- glutamic acid (C, *n*=4).** Cholesterol (11.90 g, 0.05 mol) was dissolved in dry chloroform (100 ml) and pyridine (0.2 ml) and then the mixture was added to a cold solution of *p*-phthaloyl chloride (18.30 g, 0.09 mol) in chloroform (100 ml). The reaction mixture was heated under reflux for 15 h and the solvent was removed under reduced pressure. The crude product was washed several times by a sodium hydroxide solution, then it was neutralized to pH=6. The precipitate was recrystallized from methanol, the dry white solid (5.36 g, 0.01 mol) obtained was stirred in thionyl chloride (80 ml) and dry DMF (0.2 ml) at 60°C for 3 h and then the excess thionyl chloride was removed under reduced pressure to give the corresponding acid chloride. The residue was dissolved in dry tetrahydrofuran (30 ml) and a solution of 1,4-butanediol (2.34 g, 0.026 mol) in dry tetrahydrofuran (50 ml) and pyridine (0.5 ml) was added to the flask. The reaction mixture was heated under reflux for 20 h and then excess solvent was removed under reduced pressure. The residue was washed by water first and then was recrystallized from ethanol to give compound A (5.21 g, 86%, *n*=4).

Compounds B (1.81 g, 0.007 mol) and A (1.82 g, 0.003 mol, *n*=4) in chloroform (30 ml) were heated under reflux for 12 h and then the excess solvent was removed under reduced pressure. The residue was purified by recrystallization from ethanol to obtain pure *N*-phthaloyl-L-*R*-{4-[4-(cholesteryloxycarbonyl)-benzoyloxy]- butoxy}glutamic acid C (2.44 g, 94%, *n*=4), m.p. 190.3°C. IR (KBr, $\nu$ cm$^{-1}$): 2935, 2660, 1755, 1730, 1716, 1606. $^1$ H NMR ($CDCl_3$) $\delta$: 0.94–5.43 (m, 45H), 1.58 (m, 2H), 1.76 (m, 2H), 2.41 (m, 2H), 2.49 (t, 2H), 4.37–4.86 (t, 4H), 4.66 (m, 1H), 7.77 (d, 2H, *J*=7.9 Hz), 7.79 (d, 4H, *J*=7.5 Hz), 7.83 (m, 2H), 12.45 (s, 1H). $^{13}$ C NMR ($CDCl_3$) $\delta$: 11.88, 18.73, 19.35, 21.08, 22.80, 23.85, 24.31, 25.23, 25.32, 28.02, 28.03, 28.23, 30.22, 31.62, 31.92, 35.80, 36.21, 36.68, 37.04, 38.18, 39.54, 39.77, 42.36, 50.10, 54.93, 56.19, 56.73, 62.41, 65.18, 74.20, 122.01, 122.91, 129.32, 131.31, 134.31, 140.11, 165.74, 166.71, 171.52, 173.01. Elemental analysis: calculated for $C_{52}H_{67}NO_{10}$, C 72.13, H 7.83; found, C 71.82, H 7.55%.

The yields and elemental analyses of the compound C (*n*=2, 4, 6) series are shown in table 1.

**2.2.3. GG4GC.** The glutamic acid derivative, compound C (2.90 g, 3.36 mmol, *n*=4), was stirred in thionyl chloride (10 ml) and DMF (0.1 ml) as catalyst was added. The solution was heated under reflux for 5 h whereby a clear solution was obtained. Excess thionyl chloride was removed in vacuum for 1 h. For the esterification, the acid chloride was dissolved in dry chloroform (50 ml) and pyridine (0.1 ml) and the ahydrous *a*-D-(+)-glucose (0.118 g, 0.66 mmol) was added. The reaction mixture was refluxed for 20 h in a dry $N_2$ atmosphere. After cooling back to room

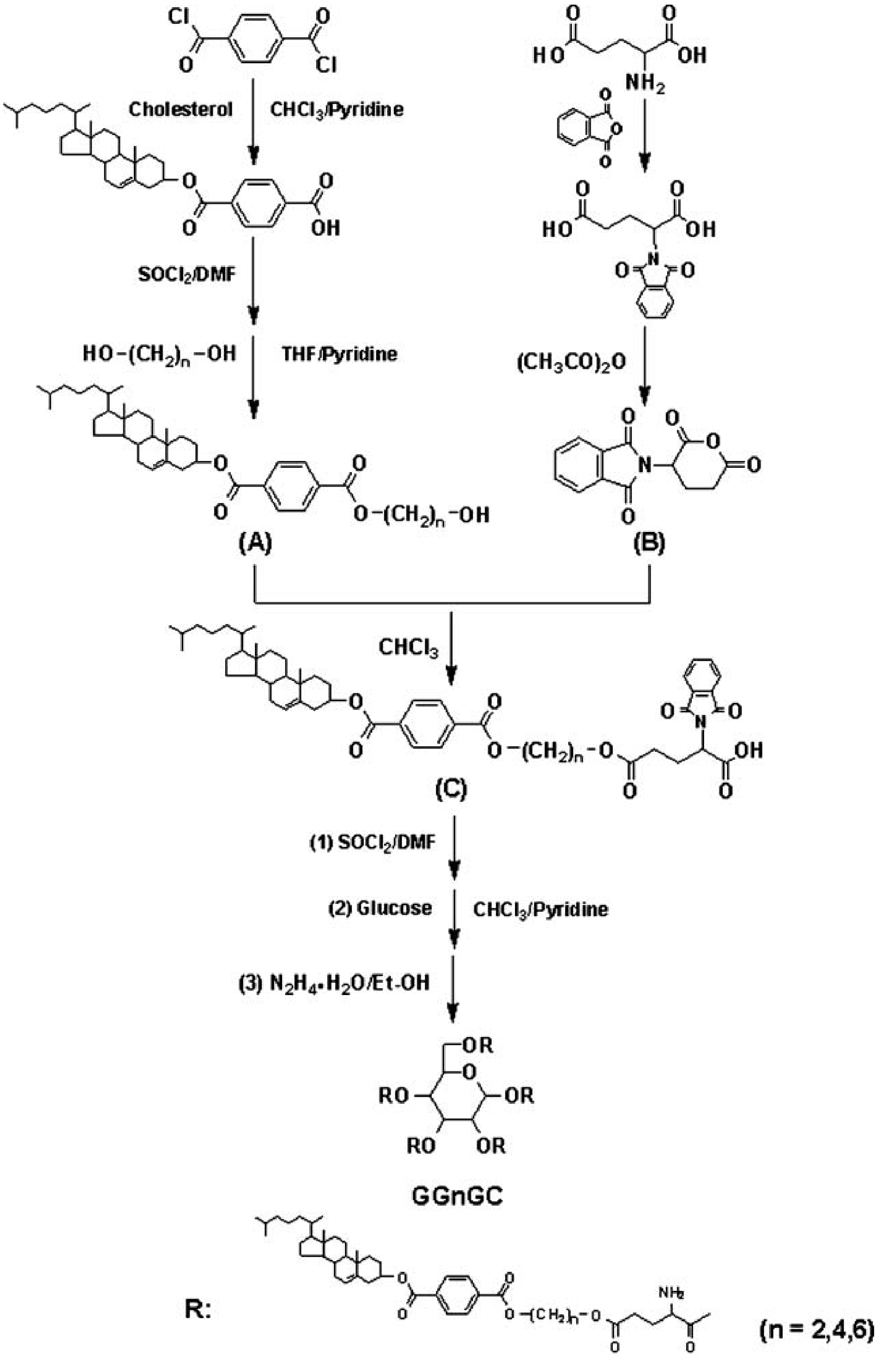

Scheme 1. Synthetic routes of GG*n*GC series.

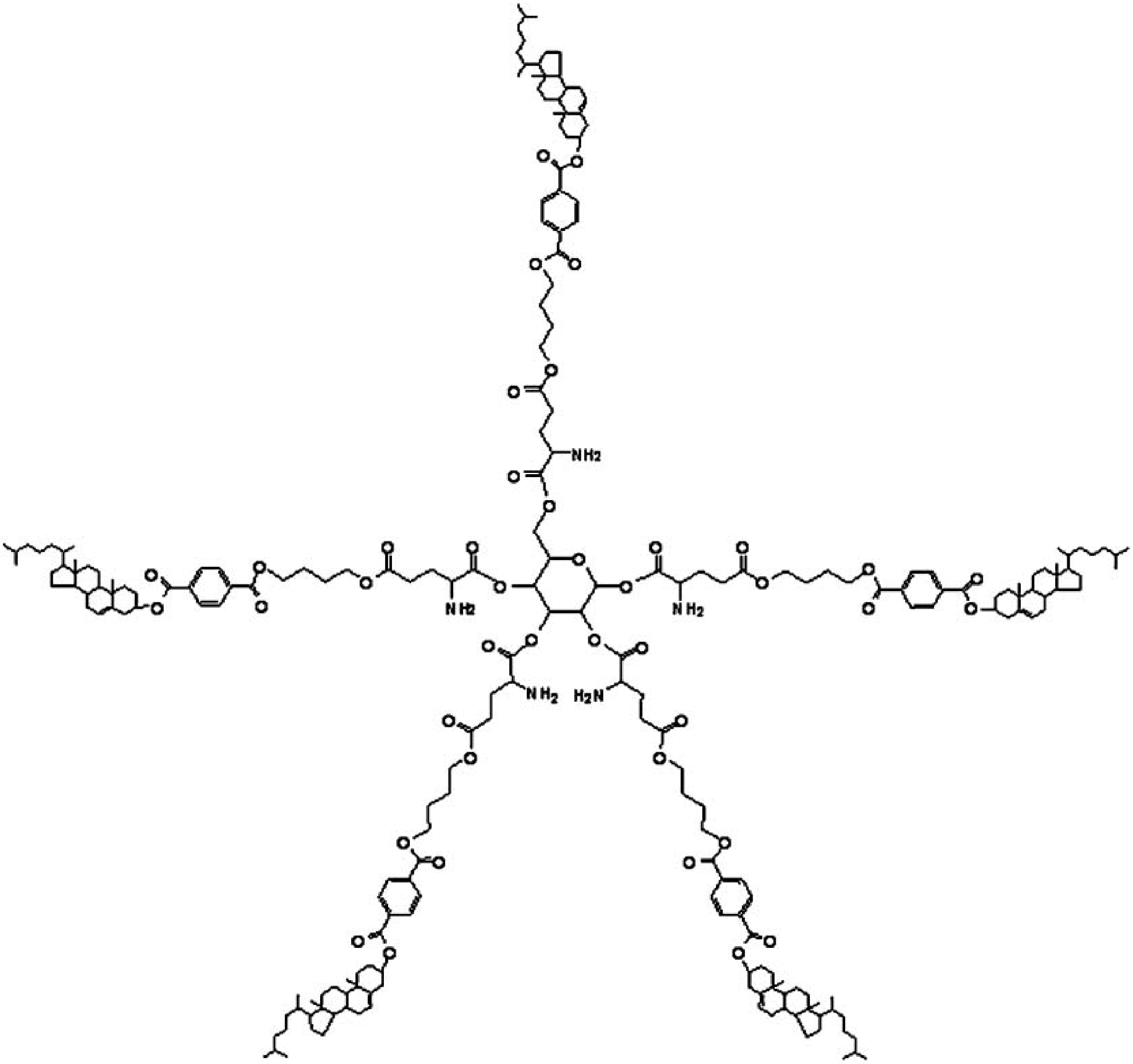

Scheme 2. Molecular structure of GG4GC.

Table 1. Yields and elemental analyses of compound C ($n$ = 2, 4, 6) series.

| Compounds C-*n* | Elemental Analyse | | | | Yields (%) |
|---|---|---|---|---|---|
| | Calcd | | Found | | |
| | C | H | C | H | |
| C-2 ($C_{50}H_{63}NO_{10}$) | 71.66 | 7.58 | 71.37 | 7.44 | 88 |
| C-4 ($C_{52}H_{67}NO_{10}$) | 72.11 | 7.80 | 71.96 | 7.61 | 79 |
| C-6 ($C_{54}H_{71}NO_{10}$) | 72.54 | 8.00 | 72.29 | 7.85 | 82 |

temperature, the mixture was poured into cold water (150 ml). The precipitate was collected by filtration and washed with distilled water. The precipitate was dried, and then the intermediate product was obtained (2.71 g, 93%).

The intermediate product (1.10 g, 0.256 mmol) was dissolved in ethanol (50 ml) and then hydrazine hydrate (0.5 ml) was added to the mixture. The reaction was refluxed for 12 h and then the solvent was completely removed under reduced pressure to give the crude product. The crude product was recrystallized from ethanol to afford a yellow solid of compound GG4GC (0.90 g, 94%), m.p. 170.3°C. IR (KBr, ν cm$^{-1}$): 3418, 2936, 1757, 1735, 1605, 1254. $^{1}$H NMR ($CDCl_3$) δ: 0.93–5.44 (m, 225H), 1.64 (m, 10H), 1.78 (m, 10H), 2.29 (m, 10H), 2.35 (t, 10H), 3.53 (m, 5H), 4.13–4.38 (t, 20H), 4.31 (d, 2H, *J*=5.7 Hz), 4.65–6.66 (m, 5H), 7.73 (d, 10H, *J*=7.6 Hz), 7.75 (d, 10H, *J*=7.8 Hz), 8.10 (d, 10H, *J*=5.5 Hz). $^{13}$C NMR ($CDCl_3$) δ: 11.82, 19.21, 19.38, 21.07, 22.82, 23.84, 24.30, 25.21, 25.53, 27.86, 28.02, 29.25, 30.01, 31.94, 32.04, 35.81, 36.20, 37.02, 37.12, 38.17, 39.53, 39.75, 42.34, 50.06, 53.33, 56.16, 56.71, 61.32, 64.43, 65.01, 69.05, 69.69, 70.09, 72.64, 75.18, 91.56, 122.96, 129.52, 134.28, 139.70, 165.91, 170.83, 171.12, 171.67, 171.97, 172.47, 173.13. Elemental analysis: calculated for $C_{226}H_{327}N_5O_{41}$, C 72.01, H 8.71; found, C 71.73, H 8.63%.

The yields and elemental analyses of the GG*n*GC (*n*=2, 4, 6) series are shown in table 2, and the configuration of the anomeric centre in the GG*n*GC series is alpha.

## 3. Results and discussion

### 3.1. *Spectroscopic analysis*

The FTIR spectrum of the representative compound, GG4GC, showed characteristic bands at 3418 cm$^{-1}$ due to azyl (–$NH_2$) stretching, 1757–1735 cm$^{-1}$ due to ester (C=O) stretching, 1605 cm$^{-1}$ due to aromatic C=C stretching and 1254 cm$^{-1}$ due to ether (C–O–C) stretching. The $^{1}$H NMR spectrum of GG4GC showed a series of multiple peaks at 0.93–5.44, 1.64–4.38, 3.53, 4.31–6.66, 7.73–7.75 and 8.10 ppm corresponding to cholesteryl, methylene, methine, glucosyl, aromatic and azyl groups. The $^{13}$C NMR spectrum of glucose derivative GG4GC showed six peaks at 61.32, 69.05, 69.69, 70.09, 72.64 and 91.56 ppm; these peaks indicated the existence of chiral core glucose. The typical five carbonyl carbon peaks at 172.47, 171.97, 171.67, 171.12 and 170.83 ppm were the characteristic peaks to judge the perfect substitution on glucose, thus ensuring that the target compound GG4GC was obtained.

### 3.2. *Thermal properties of GGnGC series LCs*

The thermal properties of the GG*n*GC series LCs were characterized by DSC. The corresponding phase transition temperatures are summarized in table 3 and the representative DSC thermograms of GG4GC are shown in figure 1. During the heating cycle, as is known, the DSC endotherm peaks of melting temperature ($T_m$) of small molecular weight LCs are sharp whereas the DSC endotherm peaks of $T_m$ of liquid crystalline polymers are flat or inconspicuous. From the DSC heating curve of GG4GC we found that the DSC endotherm peak of $T_m$ ($T_m$=170.3°C) was flat, which seemed to indicate a polymer endotherm peak, but GG4GC is not polymer. A similar phenomenon was observed in whole GG*n*GC series, which was probably due to steric hindrance. The steric effect was enforced mainly due to the hindrance contributed by the cholesteryl group, and this huge group imposed additional constraints on the motion of chain segments. Thus, the steric hindrance effect is significant in the fusion of the GG*n*GC series.

As summarized in table 3, TGA results for the GG*n*GC series show that the temperatures at which 5% weight loss occurred ($T_c$) were all higher than 250°C, which showed that the GG*n*GC series had relative high thermal stability. The relative high thermal stability is probably due to the bulky cholesteryl group in the molecular structure of the GG*n*GC series.

The target compounds showed enantiotropic behaviour, with wide mesogenic regions and high isotropic transition temperature ($T_i$). The $T_i$ involves the mobility of chain segments; it is influenced by the nature of

Table 2. Yields and elemental analyses of GG*n*GC series.

| GG*c*GC | Elemental Analyse | | | | Yields (%) |
|---|---|---|---|---|---|
| | Calcd | | Found | | |
| | C | H | C | H | |
| GG2GC ($C_{216}H_{307}N_5O_{41}$) | 71.47 | 8.53 | 71.33 | 8.41 | 95 |
| GG4GC ($C_{226}H_{327}N_5O_{41}$) | 72.01 | 8.71 | 71.73 | 8.63 | 94 |
| GG4GC ($C_{236}H_{347}N_5O_{41}$) | 72.49 | 8.94 | 72.26 | 8.75 | 92 |

Table 3. Phase transition temperatures and specific rotations of GG*n*GC series.

| GG*n*GC (*n*) | Transition temperature/°C (corresponding enthalpy changes/KJ•mol$^{-1}$) $\frac{\text{heating}}{\text{cooling}}$ | $\Delta T$[a] | $\Delta T$[b] | $\Delta T$[c] | $[a]_{589}^{20}$ (*c* 0.34, in $CHCl_3$ |
|---|---|---|---|---|---|
| 6 | K 148.2(37.0)Ch 184.6(1.45)I<br>I 180.6(−1.1)Ch 143.5[d](−)K | 36.4 | 37.1 | 259 | −379.5 |
| 4 | K 170.3(112.2) Ch 212.9(3.0)I<br>I 202.9(−2.2) Ch 162.1[d](−)K | 42.6 | 40.8 | 268 | −103.9 |
| 2 | K 171.8(84.5) Ch 220.8(2.7)I<br>I 214.8(−1.9) Ch 166.9[d](−)K | 49.0 | 47.9 | 266 | −8.3 |

K = solid, Ch = cholesteric, I = isotropic.
[a] Mesophase temperature range on first heating cycle.
[b] Mesophase temperature range on first cooling cycle.
[c] Temperature at which 5% weight loss occurred.
[d] Observed from POM.
$[a]_{589}^{20}$: Specific rotation.

molecular structure, the rigidity of the mesogenic groups and the length of flexible spacer group. It decreases with increase in the flexibility of the molecule. The $T_i$ of the GG*n*GC series decreases from 220.8°C to 184.6°C with an increase in the flexible spacer group length. Similar to $T_i$, the $T_m$ of GG*n*GC series also decreases with an increase in the flexible spacer group length, as shown in table 3. All these observations indicate that the constraint on the motion of chain segments decreases and molecular flexibility increases as the flexible spacer group is extended (*n* increased from 2 to 6).

### 3.3. *Optical properties*

The optical textures of the GG*n*GC series were studied by hot-stage POM. The POM observations showed that the GG*n*GC series exhibited a cholesteric liquid crystalline phase during both heating and cooling cycles. The phase-transition temperatures determined by DSC were consistent with POM observations. The representative optical textures of GG4GC are shown in figure 2.

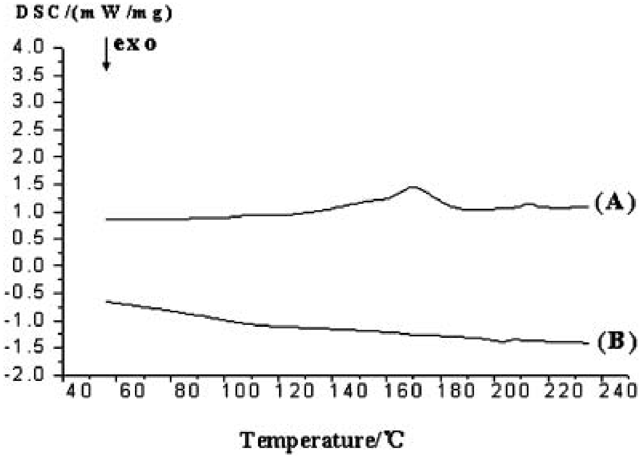

Figure 1. DSC thermograms of star-shaped liquid crystal GG4GC. (A: first heating; B: first cooling).

The unique optical properties of the GG*n*GC series are related to the helical structure of the cholesteric phase, and this helical structure can selectively reflect visible light. The helical pitch controls the wavelength of the selectively reflected light. If the helical pitch coincides with the wavelength of visible light, the cholesteric phase exhibits a brilliant colour. Due to the angular dependence of the reflection conditions, the wavelength of selective light reflection obeys the Bragg condition:

$$\lambda_m = \tilde{n} p \cos\theta, \quad (1)$$

where $\tilde{n}$ is the average refractive index of the cholesteric phase, $p$ is the pitch of the cholesteric helix and $\theta$ is the angle of incidence. When $\theta = 0°$ (normal incidence) $\lambda_m = \lambda_0 = \tilde{n}p$, the intensity of reflected light is a maximum at $\lambda_m = \lambda_0$, and falls off very rapidly on either side of $\lambda_0$ [21]. In general, the pitch decreases as temperature increases and a blue shift of the reflection wavelength is observed; when the temperature falls, the pitch increases, and a corresponding red shift of the reflection wavelength is observed.

The pitch affects not only the reflection colour, but also the optical textures of the cholesteric phase. When the pitch lies within the wavelength of visible light, the cholesteric phase exhibits planar oily-streak texture; when the pitch is much greater than the wavelength of visible light, a fingerprint texture can be observed; when the pitch is less than the wavelength of visible light, the focal-conic texture is observed. However, the focal-conic texture can easily change into oily-streak by slight shearing.

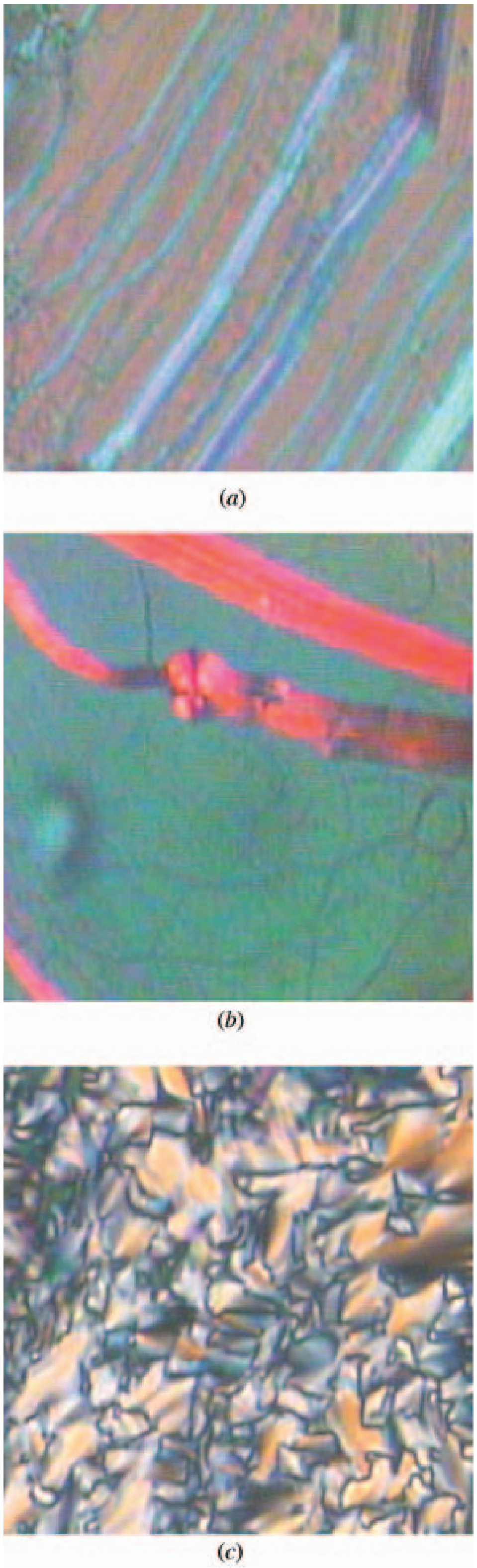

Figure 2. Optical textures of GG4GC: (a) oily-streak texture, on heating to 180°C; (b) oily-streak texture, on heating to 190°C; (c) fan-conic texture, on cooling to 199°C.

The GG*n*GC series exhibited enantiotropic oily-streak and focal-conic textures [22] and the reflection colour was observed. When the GG*n*GC series were heated to $T_m$, the obvious oily-streak texture and reflection colour appeared, the colour changed from red to green to blue between the melting temperature and the isotropic transition temperature, but the main reflection colour was blue. On cooling the sample from the isotropic melt, the focal-conic texture was formed, which readily transformed to oily-streak texture by shearing the sample, then oily-streak appeared again following the selective light reflection colour appeared.

Although the change of spacer group length did not affect mesogenic type and texture of the GG*n*GC series, a remarkable increase in SROT ($[\alpha]^{20}_{589}$, temperature: 20°C, wavelength: 589 nm) of the GG*n*GC series was observed, as summarized in table 3. The SROT increased from $[\alpha]^{20}_{589}$ $-8.3$ (ca. 0.34, in $CHCl_3$) to $[\alpha]^{20}_{589}$ $-379.5$ (*c* 0.34, in $CHCl_3$) with increase in the flexible spacer group. It indicates that the longer the spacer group, the more freedom the chain structure has and the higher the SROT value.

### 3.4. *X-ray diffraction analysis*

XRD studies were carried out to obtain more detailed information on liquid crystalline phase structure. In general, a sharp and strong peak at a low angle ($1^\circ < 2\theta < 4^\circ$) in small-angle X-ray scattering curves and a broad peak associated with lateral packing at $2\theta \approx 20^\circ$ can be observed in wide-angle X-ray diffraction curves for smectic phase structure; no peak appeared at a low angle, and a broad peak at $2\theta \approx 20^\circ$ was observed for nematic phase structure. For the cholesteric phase structure, no peak appeared at a low angle, and a broad peak occurred only at $2\theta \approx 16-18^\circ$ [23]. Representative XRD patterns of quenched GG*n*GC series samples are shown in figure 3; all of the

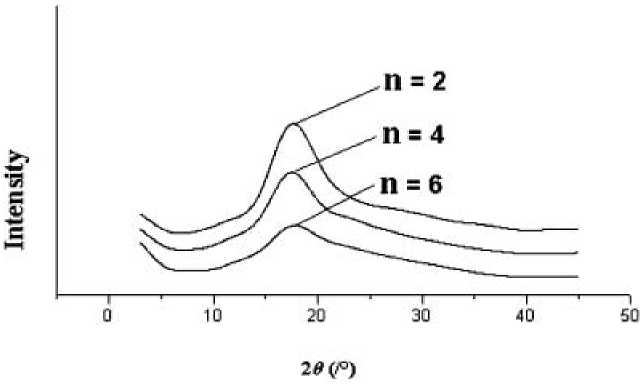

Figure 3. X-ray diffraction patterns of quenched GG*n*GC series.

compounds showed amorphous diffuse peaks at about $2\theta\approx 17.5^\circ$ ($d\approx 5.12$Å), and no sharp peak in the lower Bragg angle region was observed. Combining POM with XRD measurement may reveal that the GG*n*GC series has cholesteric phase structure.

Furthermore, the amorphous diffuse peaks of GG*n*GC series all appeared around 17.5°, but the intensity of diffuse peaks decreased as the flexible spacer group length increased (*n* increased from 2 to 6), as shown in figure 3. This observation indicated that the longer spacer group degraded the arrangement of mesomorphic units and the short-range order parameter decreases.

## 4. Conclusion

A series of star-shaped carbohydrate derivative LCs, GG*n*GC, was synthesized. The azyls in the molecular structure of the GG*n*GC series may lead to potential synthesis applications. The GG*n*GC series exhibit a wide mesogenic region and high thermal stability, which could lead to potential applications. These compounds do not have a sharp DSC endotherm peak at $T_{\mathrm{m}}$. Oily-streak and focal-conic textures were observed, which are typical cholesteric liquid crystalline textures. Both $T_{\mathrm{i}}$ and $T_{\mathrm{m}}$ decrease as the length of flexible spacer group is extended. The length of flexible spacer group plays an important role in the molecular structure and thermal properties of the GG*n*GC series, but it does not affect mesogenic type and texture of the GG*n*GC series.

## Acknowledgements

The authors are grateful to National Natural Science Fundamental Committee of China and HI-Tech Research and development programme (863) of China and National Basic Research Priorities Programme (973) of China, Science and Technology Research Major Project of Ministry of Education of China, and Specialized Research Fund for the Doctoral Programme of Higher Education for financial support of this work.

## References

[1] T.T. Chong, T. Heidelberg, R. Hashim, S. Gary. *Liq. Cryst.*, **34**, 267 (2007).

[2] V. Vill, T. Bocker, J. Thiem, F. Fischer. *Liq. Cryst.*, **33**, 1353 (2006).

[3] G. John, H. Minamikawa, M. Masuda, T. Shimizu. *Liq. Cryst.*, **30**, 747 (2003).

[4] C.M. Paleos, D. Tsiourvas. *Liq. Cryst.*, **28**, 1127 (2001).

[5] H.L. Nguyen, J. Dedier, H.T. Nguyen, G. Sigaud. *Liq. Cryst.*, **27**, 1451 (2000).

[6] D. Schwabisch, S. Wille, M. Hein, R. Miethchen. *Liq. Cryst.*, **31**, 1143 (2004).

[7] C. Zur, A.O. Miller, R. Miethchen. *Liq. Cryst.*, **24**, 695 (1998).

[8] D.F. Ewing, M. Glew, J.W. Goodby, J.A. Haley, S.M. Kelly, B.U. Komanschek, P. Letellier, G. Mackenzie, G.H. Mehl. *J. Mater. Chem.*, **8**, 871 (1998).

[9] D.F. Ewing, J.W. Goodby, J.A. Haley, S.M. Kelly, P. Letellier, G. Mackenzie. *Liq. Cryst.*, **23**, 759 (1997).

[10] J.W. Goodby, M.J. Watson, G. Mackenzie, S.M. Kelly, S. Bachir, P. Bault, P. Gode, G. Goethals, P. Martin, G. Ronco, P. Villa. *Liq. Cryst.*, **25**, 139 (1998).

[11] P. Bault, P. Gode, G. Goethals, J.W. Goodby, J.A. Haley, S.M. Kelly, G.H. Mehl, G. Ronco, P. Villa. *Liq. Cryst.*, **25**, 31 (1998).

[12] P. Sakya, J.M. Seddon, V. Vill. *Liq. Cryst.*, **23**, 409 (1997).

[13] V. Vill, H.W. Tunger, D. Peters. *Liq. Cryst.*, **20**, 547 (1996).

[14] H. Kuttenreich, H.J. Hinz, R.D. Koynova, R.D.B.G. Tenchov. *Chem. Phys. Lipids*, **66**, 55 (1993).

[15] R.N.A.H. Lewis, D.A. Mannock, R.N. McElhaney, P.T.T. Wong, H.H. Mantsch. *Biochemistry*, **29**, 8933 (1990).

[16] B. Pfannemuller, W. Welte, E. Chin, J.W. Goodby. *Liq. Cryst.*, **33**, 1238 (2006).

[17] V. Vill, J. Thiem. *Liq. Cryst.*, **9**, 451 (1991).

[18] N.L. Morris, R.G. Zimmermann, G.B. Jameson, A.W. Dalziel, P.M. Reuss, R.G. Weiss. *J. Am. Chem. Soc.*, **110**, 2177 (1988).

[19] S. Seo, Y. Tomita, K. Tori, Y. Yoshimura. *J. Am. chem. Soc.*, **100**, 3331 (1978).

[20] P. Allevi, M. Anastasia, P. Ciuffreda, A. Fiecchi, A. Scala. *Chem. Phys. Lipids*, **53**, 219 (1990).

[21] P. Das, J. Xu, J. Roy. *J. chem. Phys.*, **111**, 8240 (1999).

[22] I. Dierking. . In, *Textures of Liquid Crystals*, I. Dierking (Eds), pp. 51, Wiley-VCH, Weinheim (2003).

[23] B.Y. Zhang, Y.G. Jia, J.S. Hu, F.B. Meng. *Liq. Cryst.*, **31**, 387 (2004).